Synthesis of (E)-Ethyl-4-(2-(furan-2-ylmethylene)hydrazinyl)benzoate, crystal structure, and studies of its interactions with human serum albumin by spectroscopic fluorescence and molecular docking methods

Miguel Morales-Toyo, Christopher Glidewell, Julia Bruno-Colmenares, Néstor Cubillán, Ronald Sánchez-Colls, Ysaias Alvarado, Jelen Restrepo

PII: S1386-1425(19)30266-5
DOI: https://doi.org/10.1016/j.saa.2019.03.028
Reference: SAA 16918
To appear in: *Spectrochimica Acta Part A: Molecular and Biomolecular Spectroscopy*
Received date: 5 December 2018
Revised date: 11 March 2019
Accepted date: 11 March 2019

Please cite this article as: M. Morales-Toyo, C. Glidewell, J. Bruno-Colmenares, et al., Synthesis of (E)-Ethyl-4-(2-(furan-2-ylmethylene)hydrazinyl)benzoate, crystal structure, and studies of its interactions with human serum albumin by spectroscopic fluorescence and molecular docking methods, Spectrochimica Acta Part A: Molecular and Biomolecular Spectroscopy, https://doi.org/10.1016/j.saa.2019.03.028

Synthesis of (*E*)-Ethyl-4-(2-(furan-2-ylmethylene)hydrazinyl)benzoate, Crystal Structure, and Studies of Its Interactions with Human Serum Albumin by Spectroscopic Fluorescence and Molecular Docking Methods.

Miguel Morales-Toyo,[1,2*] Christopher Glidewell,[3] Julia Bruno-Colmenares,[4] Néstor Cubillán,[5] Ronald Sánchez-Colls,[6] Ysaias Alvarado,[1,7] Jelen Restrepo.[6**]

[1]Laboratorio de Electrónica Molecular (LEM), Departamento de Química, Facultad Experimental de Ciencias, La Universidad del Zulia, Ap. 526, Grano de Oro, Módulo No. 2, Maracaibo, Estado Zulia, Bolivarian Republic of Venezuela.

[2]Facultad de Ciencias, Universidad Adventista Dominicana (UNAD), Autopista Duarte Km 74 ½, Villa Sonador, Provincial Monseñor Nouel, 42000, República Dominicana.

[3]School of Chemistry, University of St Andrews, St Andrews, Fife KY16 9ST, UK.

[4]Materials Laboratory for Emerging Technologies (LaMTE), Center for Research in Materials Technology (CITeMA), Venezuelan Institute of Scientific Research (IVIC), Bolivarian Republic of Venezuela.

[5]Programa de Química, Universidad del Atlántico, Barranquilla, Colombia.

[6]Laboratory of Sustainable Synthesis of New Materials. Center for Research in Materials Technology (CITeMA), Venezuelan Institute of Scientific Research (IVIC), Bolivarian Republic of Venezuela.

[7]Laboratory of Molecular and Biomolecular Characterization, Center for Research in Materials Technology (CITeMA), Venezuelan Institute of Scientific Research (IVIC), Bolivarian Republic of Venezuela.

Emails: *miguelmorales@unad.edu.do; **jrestrepo@ivic.gob.ve

Abstract

A novel hydrazone, (*E*)-Ethyl-4-(2-(furan-2-ylmethylene)hydrazinyl)benzoate (EFHB), has been synthesized and characterized by FT-IR, NMR and Mass spectroscopy, and X-ray diffraction; compound crystallized as translucent light yellow thin plates. EFHB was studied for their binding to human serum albumin (HSA) using the fluorescence quench titration method. Molecular docking was also performed to get a more detailed insight into their interaction with HSA at the binding site. Addition of this hydrazone to HSA

produced significant fluorescence quenching and splitting of emission spectra of HSA through static quenching mechanism with binding constants of about 10^4 M^{-1} at 292.15, 298.15, 304.15 and 310.15 K. According to the synchronous fluorescence, tryptophan and tyrosine residues of the protein are most perturbed by the binding process. Thermodynamic parameters ΔG, ΔH, and ΔS were got and the main sort of acting force between EFHB and HSA was studied. Results of molecular docking have shown that EFHB binds to subdomain IIA of HSA mainly by hydrophobic interaction, energy binding are in good agreement with those obtained by fluorescence study (ΔG_{the} = -7.32 ± 0.09 kcal mol^{-1} and ΔG_{exp} = -6.76 ± 0.03 kcal mol^{-1}).

Keywords: Hydrazone derivative, crystal structure, HSA, molecular docking, fluorescence spectroscopy.

1. Introduction

Hydrazones and their derivatives have been under study for a long time due to their ease preparation, increased hydrolytic stability relative to imines, and its tendency toward crystallinity. In addition, this kind of compound is a versatile class to building blocks for the synthesis of heterocyclic compounds, drug design, as possible ligands for metal complex. Have shown potential applications due to their broad spectrum of biological activity, including antitumor, antiviral, vasodilators, antimalarial, anti-inflammatory, analgesic, anticonvulsants activities.[1–3]

In the literature, synthesis of hydrazone derivatives has been reported in order to study their mechanisms of interaction with biomolecules of pharmacological interest such as human serum albumin (HSA) and bovine serum albumin (BSA), using different spectroscopic techniques and methods of molecular modeling. The interaction between the hydrazone derivatives *N*′-(2,4-dimethoxybenzylidene)-2-hydroxybenzohydrazide (DBH), 4-chloro- *N*′-(pyridin-2-ylmethylene)benzohydrazide (CPBH), 2-hydroxy-N′-(3-hydroxybenzylidene) benzohydrazide (HHB), *N*′-(4-bromobenzylidene)-2-hydroxybenzohydrazide (BBH), *N*′-benzylidene-2-hydroxybenzohydrazide (BH) and HSA/BSA have been investigated systematically by fluorescence, These hydrazone derivatives form stable complexes with HSA and BSA with binding constants of 10^4-10^5 L mol^{-1}.[4–7]

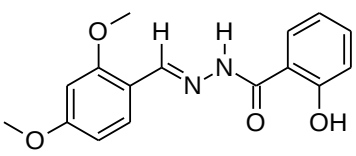

(DBH)

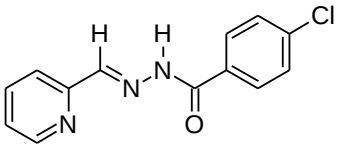

(CPHB)

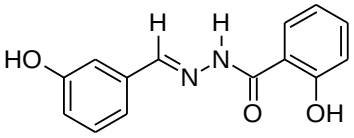

(BBH)

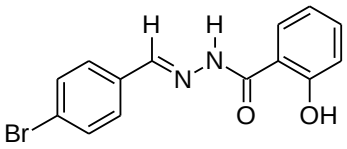

(HHB)

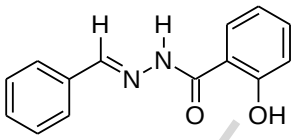

(BH)

HSA in the major protein in human bloodstream and accounts for almost 60% of total plasma protein content. HSA is composed of a single polypeptide chain containing 585 amino acids residues, is stabilized by 17 disulphide bridges, and has a molecular weight of 66 kDa. Serum albumin functional activity is essential for maintaining normal tissue and organ homeostasis, HSA is the main transporting protein for ligands due to its ability to bind to a broad range of both hydrophobic and hydrophilic molecules, including drugs (endogenous and exogenous ligands present in blood).[8–11] HSA, is a key regulator of fluid movement between plasma and interstitial compartments under physiological conditions.[12] Due to these characteristics, HSA is generally used as an important model protein in the various studies of biophysics and biochemistry, and one of the techniques used is measurement of quenching of albumin's natural fluorescence by drugs for its high sensitivity, rapidity and ease of implementation.[13,14]

In this article, we report the synthesis and molecular structure of novel hydrazone EFHB, together with biophysical studies of its interaction with HSA by fluorescence spectroscopy and molecular modeling methods.

2.- Experimental Methods

2.1. Chemicals.

The Western Hematological Institute and Blood Bank of Zulia State, Bolivarian Republic of Venezuela supplied human serum albumin (HSA). All other chemicals used were of analytical reagent grade.

2.2. Apparatus.

Melting point was determined on a digital IA-9100 ELECTROTHERMAL Fusiometer. IR spectrum was recorded on a Shimadzu FTIR-Prestige21 (IR) spectrophotometer, as KBr pellets. Spectrophotometer NMR "Brukerbiospin 500" (500 MHz ^{1}H y 125 MHz ^{13}C polinuclear) using TMS like reference patron. Mass spectrophotometer Thermo, model TQS (quadrupole triple). X-ray diffractometer "Bruker Kappa Apex II Duo", with double wavelength (Cu Ka(alfa) = 1.54; MoKa = 0.71) graphite monochromator and area detector. UV-vis spectrometer Shimadzu model UV-3101PC with multi-chamber compartment and temperature control by Peltier effect. Fluorescence measurements were made on a Shimadzu RF-5301PC Fluorospectrophotometer equipped with xenon lamp source and 1.0cm*1.0cm*4.0cm quartz cell and a thermostat bath.

2.3. Synthesis of EFHB.

In a 100 mL round bottom flask, 1.24 g (4.62 mmol) of ethyl 4-hydrazinylbenzoate hydrochloride (1) was dissolved in 50 mL of distilled water under magnetic stirring. Then, 460 µL (5.54 mmol) of furan-2-carbaldehyde (2) were added slowly, stirring for about 20 min after the addition of the furan-2-carbaldehyde (2) (Scheme 1). The product was collected by filtration, washed with two aliquots of 10mL 0.1 M HCl and then with 20 % $NaHSO_3$. The product was recrystallized in ethanol.[15]

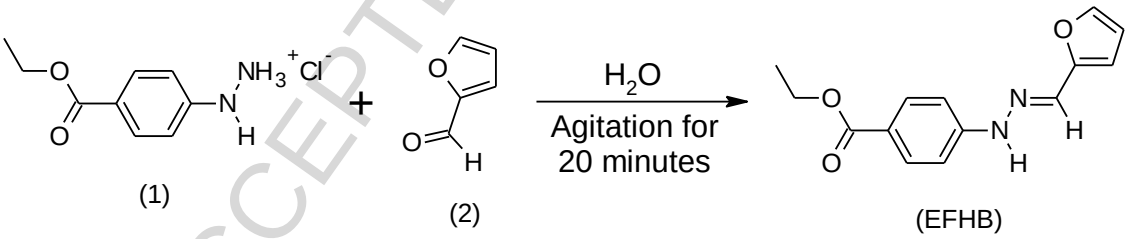

Scheme 1. Synthesis of EFHB.[16]

2.4. X-ray single-crystal crystallography.

Crystal data, data collection and structure refinement details are summarized in Table 1: standard software was used throughout.[17–19] All H atoms were located in difference maps. The H atoms bonded to C atoms were then treated as riding atoms in geometrically idealised positions with C-H distances 0.93 Å (alkenyl, aromatic and furanyl), 0.96 Å ($-CH_3$) or 0.97Å ($-CH_2-$), and with $U_{iso}(H) = kUeq(C)$, where k = 1.5

for the methyl group, which was permitted to rotate but not to tilt, and 1.2 for all other H atoms bonded to C atoms. For the H atom bonded to atom N41, the atomic coordinates were refined with $U_{iso}(H) = 1.2U_{eq}(N)$, giving an N-H distance of 0.857(18) Å.

Table 1. Crystal data and refinement for compound EFHB.

EFHB	
Crystal data	
Chemical formula	$C_{14}H_{14}N_2O_3$
M_r	258.27
Crystal system, space group	Monoclinic, $P2_1/c$
Temperature (K)	296
a, *b*, *c* (Å)	8.3132 (2), 22.8241 (5), 7.4106 (2)
β (°)	106.359 (1)
V (Å^3)	1349.17 (6)
Z	4
Radiation type	Cu $K\alpha$
μ (mm^{-1})	0.75
Crystal size (mm)	0.51 × 0.48 × 0.18
Data collection	
Diffractometer	Bruker *APEX*-II CCD
Absorption correction	Multi-scan *SADABS* (Bruker, 2009)
T_{min}, T_{max}	0.698, 0.874
No. of measured, independent and observed [$I > 2\sigma(I)$] reflections	7333, 1967, 1729
R_{int}	0.024
θ_{max} (°)	59.6
$(\sin \theta/\lambda)_{max}$ (Å^{-1})	0.559
Refinement	
$R[F^2 > 2\sigma(F^2)]$, $wR(F^2)$, S	0.035, 0.098, 1.05
No. of reflections	1967

No. of parameters	176
H-atom treatment	H atoms treated by a mixture of independent and constrained refinement
$\Delta\rangle_{max}$, $\Delta\rangle_{min}$ (e Å^{-3})	0.12, -0.19

2.5. Sample preparation and fluorescence quenching measurements.

An assay solution were prepared by adding appropriate amount HSA in Britton-Robinson buffer pH = 7.4, the concentration of HSA was determined by UV-vis spectroscopy using its molar absorptivity ε_{280} = 35219 cm^{-1} M^{-1}.[10,20,21] Ligand EFHB was dissolved in 50% w/v polyethylene glycol (PEG 3350, see figure S1, Supporting information). A solution of 2500 µL of [HSA] = 5.0 x 10^{-6} mol L^{-1} was added in a 1 cm cell and then titrated with successive additions of [EFHB] = 3.37 x 10^{-4} mol L^{-1} (10 aliquots of 20 µL each until obtaining a volume of a total solution of 2700 µL**)**. For each addition of EFHB the resulting solution was stirred for 5 minutes before measuring to reach equilibrium. Fluorescence emission spectra were measured at different temperatures (292.15, 298.15, 304.15 and 310.15 K) and recorder in the wavelength range 290-500 nm by exciting HSA at 283 nm. Excitation and emission slits were 5 nm, the white correction was carried out by subtracting the emission spectrum form the medium used (Britton-Robinson buffer pH = 7.4).[10,21,22]

2.6. Molecular Docking.

Molecular docking study was carried out using AutoDock Vina to calculate the possible conformation of the ligand EFHB into HSA, and the graphical user interface Auto-DockTools (ADT 1.5.6).[23] The X-ray crystallography structure of HSA (PDB ID: 2BXM) it was obtained from the Protein Data Bank.[24] All water and ligands molecules present in the biomolecule were removed. Polar hydrogen's were added to the protein structure using AutoDockTools (ADT). To recognize the binding sites in HSA, docking was performed by using a box size of 12x22x12 Å with 1 Å grid spacing.[24] Cluster analysis was applied on the docked results using a rmsd-tolerance of 2.0 Å. ADT program was used to analyze amino acid residues involved in the binding between HSA and EFHB, in the best binding site.[24,25] The structure of EFHB was generated by ChemSketch package.[16] The geometry of the ligand was

optimized without restriction of symmetry by semiempirical methods using the Hamiltonian PM6 implemented in the software Gaussian03W (Version B.03).[19,20]

3. Results and discussion

3.1. Synthesis and spectroscopic characterization of EFHB.

The compound EFHB was synthesized from the condensation between the ethyl 4-hydrazinylbenzoate hydrochloride (1) and furan-2-carbaldehyde (2) (Scheme 1) as described above (section 2.3). Yield = 80%, translucent light yellow plates, m.p. = 168-172 ºC. FT-IR (KBr) cm^{-1}: 3259.5 (NH); 1701.1 (C=O); 1678.0 (N=C), 1598.9 (C=C); 1305.7 (C-O-C); ^{1}H NMR (DMSO-d6, 500 MHz): δ 1.28 (t, 3H, -CH_3); 4.21 (q, 2H, -CH_2-); 6.57 (dd, 1H, J_1 = 3.4, J_2 = 1.4 Hz, H44); 6.73 (d, 1H, J = 3.4 Hz, H43); 7.03 (d, 2H, J = 8.8 Hz, H3 and H5); 7.74 (d, 1H, J = 1.4 Hz, H45); 7.81 (d, 2H, J = 8.8 Hz, H2 and H6); 7.84 (s, 1H, N=C-H); 10.80 (s, 1H, N-H); ^{13}C NMR (DMSO-d6, 125 MHz,): δ 14.3; 59.8; 110.5; 111.2; 111.9; 119.4; 129.7; 130.9; 143.8; 148.8; 150.2; 165.6; MS: M + 1 = 259.11.

3.2. Structure description.

The non-H atoms in the molecule of EFHB (Figure 1) are very nearly coplanar. For the atoms in the portion between atom N41 and atom C13, the rms deviation from their mean plane is 0.056 Å, with the maximum individual deviation being 0.1073 (14) Å for atom C13: for the portion of the molecule between atom N41 and the furanyl ring, the rms deviation from their mean plane is only 0.018 Å, with the largest individual deviation of 0.0238(13) Å for atom C42. The dihedral angle between the mean planes through these portions of the molecule is 7.16(7)^{o}. The bond lengths and angles present no unusual values: all are consistent with the corresponding values found for 22 examples of phenylhydrazones found in the Cambridge Structural Database (CSD) [28]. There is a short intramolecular C-H...O contact but this cannot be regarded as a hydrogen bond as the C-H...O angle is only 100^{o}, so that the interaction energy is likely to be negligible [29]: in addition the ethyl O atom O12 is likely to be, at best, a rather weak acceptor.

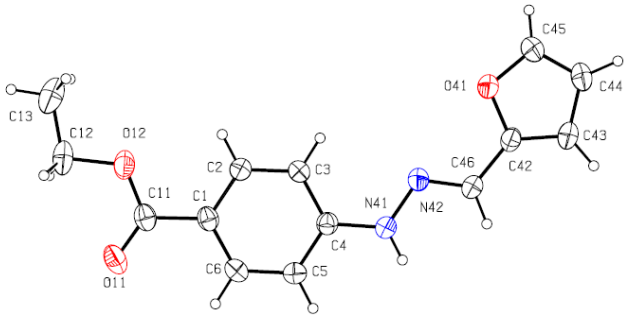

Figure 1. The molecular structure of EFHB showing the atom-labelling scheme. Displacement ellipsoids are drawn at the 30% probability level.

The 2-thienyl analogue of EFHB (CSD refcode XIGHUS) is in fact isomorphous with EFHB, with a volumetric isostructurality index value of 97.7% [15,28,30]: in addition XIGHUS turns out to exhibit exactly, the same pattern of supramolecular aggregation as found here for EFHB (see below). The supramolecular assembly of EFHB depends upon three hydrogen bonds, one each of N-H...O, C-H...O and C-H...π(arene) types (Table 2).

Table 2. Parameters (Å, ^{o}) for hydrogen bonds and short intramolecular contacts.

D-H	H…A	D…A	D-H…A	Motif
C2-H2…O12	0.93	2.41	2.7261(18) 100	S(5)
N41-H41...O11[a]	0.857(18)	2.075(18)	2.9068(17) 164.2(13)	C(8)
C46-H46...O11[a]	0.93	2.57	3.3460(18) 141	C(10
C6-H6...Cg1[b]	0.93	2.94	3.6237(15) 131	-

Cg1 represents the centroid of the ring (C1-C6). Symmetry codes: a (1 + x, 0.5 - y, 0.5 + z), b (x, 0.5 - y, -0.5 + z).

The N-H...O and C-H...O hydrogen bonds together link molecules related by a glide plane to form a C(8)C(10)[R^1_2(6)] chain of rings running parallel to the [201] direction (Figure 2) [31]. In addition, the C-H...π(arene) hydrogen bond links molecules also related by a glide plane into a chain running parallel to the [001] direction (Figure 3), and the combination of these two chain motifs generates a sheet lying parallel to (010) (Figure 4), but there are no direction-specific interactions between adjacent sheets.

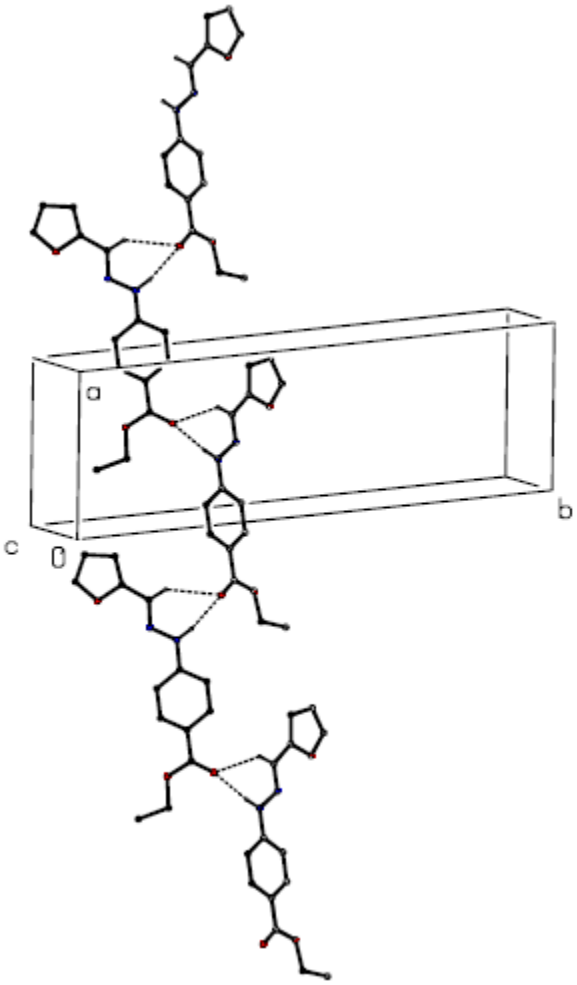

Figure 2. Part of the crystal structure of EFHB sowing the formation of a chain of rings built from N-H...O and C-H...O hydrogen bonds and running parallel to the [201] direction. Hydrogen bonds are shown as dashed lines and, for the sake of clarity, the H atoms not involved in the motif shown have been omitted.

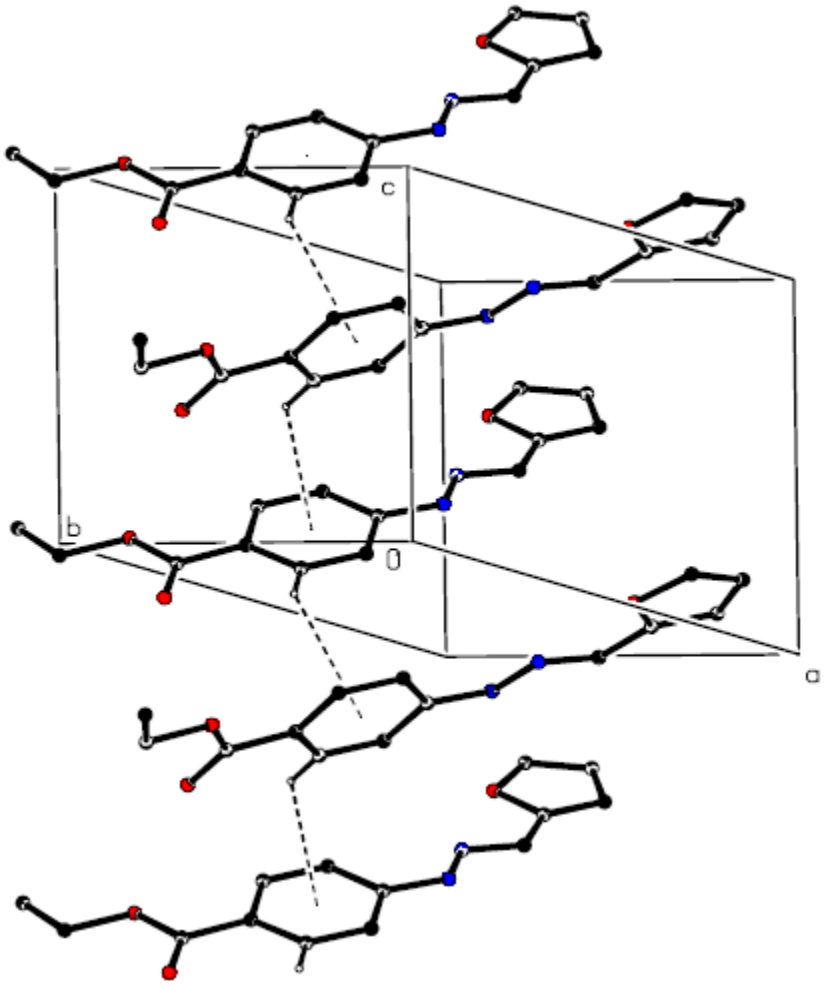

Figure 3. Part of the crystal structure of EFHB sowing the formation of a chain built from C-H...π(arene) hydrogen bonds and running parallel to the [001] direction. Hydrogen bonds are shown as dashed lines and, for the sake of clarity, the H atoms not involved in the motif shown have been omitted.

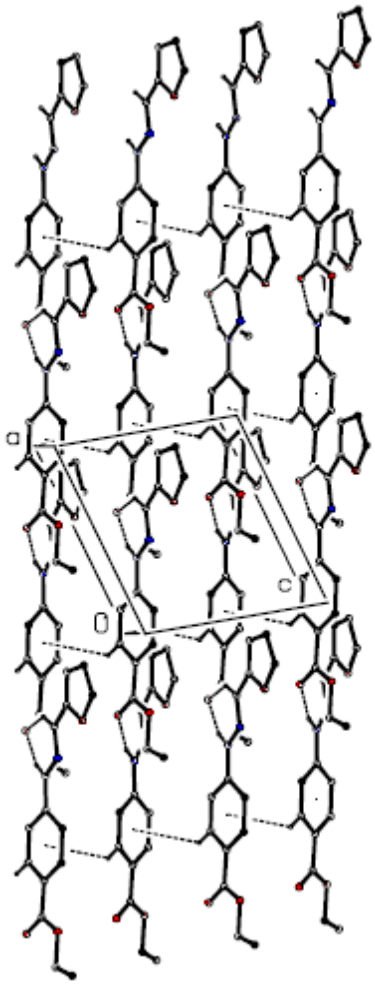

Figure 4. Part of the crystal structure of EFHB sowing the formation of a sheet built from N-H...O, C-H...O and C-H...π(arene) hydrogen bonds and lying parallel to (010). Hydrogen bonds are shown as dashed lines and, for the sake of clarity, the H atoms not involved in the motifs shown have been omitted.

3.3. Interaction between EFHB and HSA: Influence on the fluorescence spectrum.

Fluorescence spectroscopy is widely used to determine the nature of the interactions between ligands and biomolecules. This technique allows determining the mechanism by which the HSA-Ligand association is generated, distances bond of the complex, the magnitudes of the association constants and thermodynamic parameters.

HSA possesses within its molecular structure three kinds of residues of amino acids or fluorophores: one residue tryptophan (Trp), eighteen residues of tyrosine (Tyr) and thirty-one residues of phenylalanine (Phe). The intrinsic fluorescence of the HSA is mainly due to the Trp residue, this biomolecule possesses only one (Trp214), which is located in the hydrophobic cavity, subdomain IIA (site I). Fluorescence of Tyr is almost

completely quenched for many proteins in their native states because it is dissociated or in the presence of amine groups, carboxylate groups, carboxylic acids or Trp residues. Phe possesses the property of emitting fluorescence, however, lacks practicality because it possesses a very low quantum yield.[8,9]

Binding of EFHB to HSA was monitored by the change in intrinsic fluorescence phenomenon of HSA (fluorophore) in the absence and presence of EFHB (quencher). In the present investigation, HSA was excited at a wavelength 283 nm (λ_{ex} = 283 nm) and the maximum fluorescence emission (λ_{max}) was observed at 341 nm (Figure 5). With increasing concentrations (0-2.5 x 10^{-6} mol L^{-1}) of EFHB, the fluorescence intensity of HSA (5.0 x 10^{-6} mol L^{-1}) was gradually decreased or quenched.[10]

All the fluorescence data are corrected for absorption of exciting light (283 nm) and emitted light (341 nm) according relationship:

$$F_c = F_m \, e^{(A_1+A_2)/2} \qquad (1)$$

F_c and F_m are the corrected and measured fluorescence, respectively. A_1 and A_2 are the absorbance of EFHB at excitation wavelength and emission wavelength, respectively.[32–34]

Figure 5 shows the fluorescence emission spectrum of the HSA in the absence (spectrum A) and in the presence of EFHB at different concentrations (B-K spectra) and 298.15 K of temperature. HSA has a fluorescence emission spectrum with a maximum at wavelength of 341 nm in the absence of the ligand, in this graph we can watch clearly a decrease in the intensity of the intrinsic emission fluorescence of HSA, with quenching HSA fluorescence a hypsochromic displacement of the emission band of 341 at 316 nm is produced. In addition, a splitting of the emission band is generated which results in the formation of a new emission band at 387 nm.

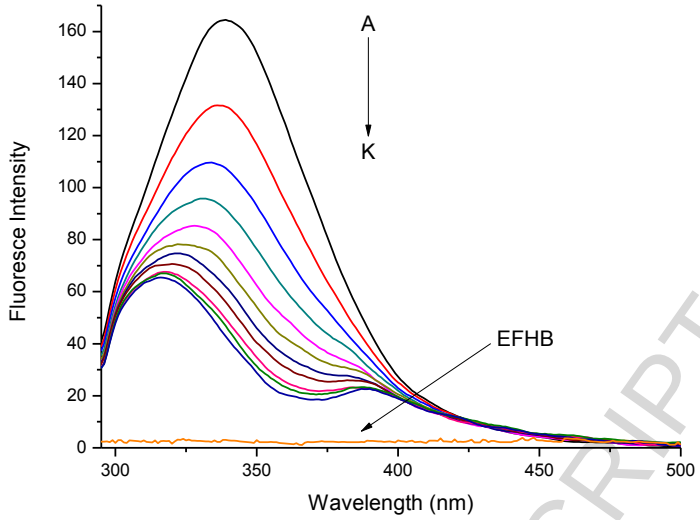

Figure 5. Effect of EFHB on the fluorescence emission spectrum of HSA in Britton-Robinson buffer of pH = 7.4 at 298.15 K. The concentration of EFHB: A) 0.0 mol L^{-1}, B) 2.7 x 10^{-6} mol L^{-1}, C) 5.3 x 10^{-6} mol L^{-1}, D) 7.9 x 10^{-6} mol L^{-1}, E) 1.0 x 10^{-5} mol L^{-1}, F) 1.3 x 10^{-5} mol L^{-1}, G) 1.5 x 10^{-5} mol L^{-1}, H) 1.8 x 10^{-5} mol L^{-1}, I) 2.0 x 10^{-5} mol L^{-1}, J) 2.3 x 10^{-5} mol L^{-1}, K) 2.5 x 10^{-5} mol L^{-1}; the concentration of HSA is 5.0 x 10^{-6} mol L^{-1}.

Abou-Zied and Al-Lawatia, reported the characterization of the binding site of a series of hydroxyquinolines (HQs) in HSA and found that these kinds of systems presented similar spectral behaviors to those found in this work; Displacements and splitting of emission band of HSA were evidenced. According to the researchers, these findings were generated as a consequence of selective quenching of Trp214 in HSA by the HQs ligands, these quenching in the emission fluorescence produce the unmasking of the fluorescence of the Tyr residues.[9]

HSA has in its molecular structure eighteen residues of Tyr, it is important to note that only one of these residues Tyr (Tyr263) and Trp214 are in the pocket IIA (site I). These investigators estimated the distances between Tyr residues and Trp214 from the crystalline structure of the HSA, finding that the distances between Tyr-Trp residues are in the range of 13-35 Å and about 17 Å for the distance Tyr263-Trp214. The critical distance at which the 50% energy transfer takes place is 15 Å. Therefore, the probability that an energy transfer occurs between the Tyr263-Trp214 residues is high. Thus, upon selective quenching of Trp214, fluorescence emission of the Tyr263 residue will no

longer be masked and its emission band at a lower wavelength with respect to the maximum emission band of the native HSA can be visualized.[35–37]

The results obtained in this work, suggest that the unmasking of the Tyr263 fluorescence takes place at a wavelength of 316 nm (Figure 5), as a consequence of the selective quenching of the fluorescence emission of Trp214 in the HSA-EFHB system.[8]

3.4. Synchronous fluorescence study of EFHB on the Fluorescence Spectrum of HSA.

Synchronous fluorescence is utilized to characterize the interaction of ligands with proteins; with this technique, we can obtain information about the molecular microenvironment of the chromophores in the biomolecule. Generally, the difference between the emission wavelength and the excitation wavelength ($\Delta\lambda$), reflects the spectral nature of the chromophores. When $\Delta\lambda$ = 60 nm, the synchronous fluorescence spectrum of HSA is characteristic of the Trp residue, whereas when $\Delta\lambda$ = 15 nm is characteristic of the emission of Tyr residues.[38]

The intensities of the fluorescence emission spectra for the Trp and Tyr residues in the synchronous fluorescence assays are quenched when the concentration of the EFHB ligand gradually increases. Maximum in the emission spectrum of Trp residue changes from 283 to 280 nm (Figure S2, Supporting information), and the maximum emission spectrum of the Tyr changes slightly from 288 to 286 nm (Figure S3, Supporting information), these spectral changes towards shorter wavelengths (hypsochromic effect) suggest that the polarity in the environment of Trp and Tyr decreases, making the cavity that harbors them more hydrophobic and they are less exposed to the solvent when the HSA comes into contact with the EFHB ligand.[39,40]

3.5. HSA fluorescence quenching mechanism.

The Stern-Volmer equation (Equation 2) it was employed to determine the HSA quenching mechanism in presence of the ligand EFHB.[41] Equation 2 describes a straight line when graphing the F_0/F ratio as a function of [Q] at different temperatures; this implies that the mechanism of quenching the intrinsic fluorescence of a

biomolecule occurs through a homogeneous process, a static or dynamic mechanism.[20,41]

$$\frac{F_o}{F} = 1 + K_{SV}[Q] = 1 + k_q \tau_o [Q] \qquad (2)$$

F_0 and F are the fluorescence intensities of the biomolecule in the absence and presence quencher respectively, K_{SV} is the Stern-Volmer quenching constant, [Q] is the molar concentration of quencher, k_q is the quenching rate constant of biological macromolecule, τ_0 is the average excited state lifetime of HSA without quencher, that is, 5.78 x 10^{-9} s.[20] By plotting the relation of the fluorescence F_0/F against the [Q] a straight line is obtained whose slope corresponds to the value of K_{SV} (Figure 6).[10,22]

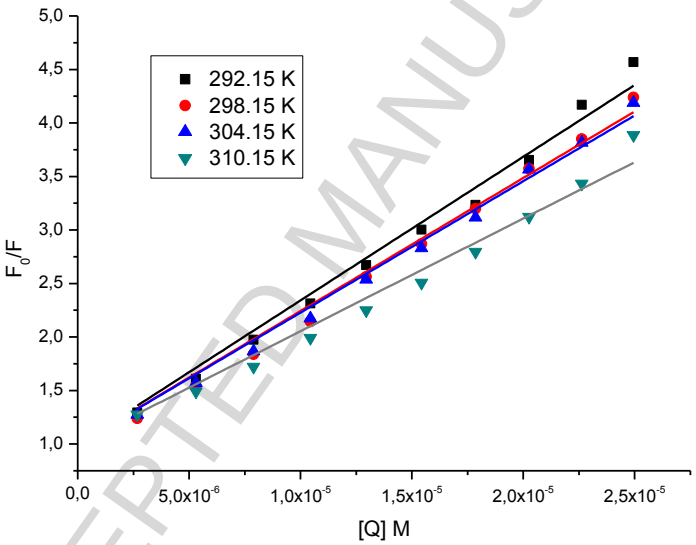

Figure 6. Stern-Volmer plots of EFHB at various temperatures.

In order to define the HSA quenching mechanism, the dependence of K_{SV} on the temperature it was evaluated, in the Table 3 it is observed that the value of K_{SV} decreases with the increase of the temperature, this tendency can also be observed in Figure 6. Therefore, the mechanism of quenching of the HSA fluorescence in the presence of EFHB is static, and is due to the formation of a complex, if the temperature increases, the value of K_{SV} will decrease because of the weakening of the non-specific and specific van der Waals forces place to the formation of the complex. On the other hand, the values of the quenching bimolecular constants k_q can be estimated from to the relation $k_q = K_{SV}/\tau_0$. This values of k_q exceed the value of the controlled collision

constant, which is 2.0 x 10^{10} M^{-1} s^{-1}.[20,34] In the present work, the value of k_q for HSA-EFHB system is greater than the limiting diffusion rate constant of the biomolecule, which indicates that the probable quenching mechanism of HSA in the presence of EFHB is initiated by ground state complex formation rather than by dynamic collision (Table 3).[22,42]

Table 3. Binding parameters of HSA-EFHB complex at 292.15, 298.15, 304.15 and 310.15 K obtained from fluorescence quenching experiments.

Fluorescence quenching experiments parameters	**292.15 K**	**298.15 K**	**304.15 K**	**310.15 K**
K_{SV} (Stern-Volmer constant, M^{-1})	13.81 ± 0.47 x 10^4	12.63 ± 0.20 x 10^4	12.31 ± 0.11 x 10^4	10.63 ± 0.08 x 10^4
k_q (bimolecular quenching rate constant, M^{-1} s^{-1})	2.39 ± 0.08 x 10^{13}	2.18 ± 0.03 x 10^{13}	2.13 ± 0.02 x 10^{13}	1.84 ± 0.01 x 10^{13}
K_a (binding constant, M^{-1})	10.05 ± 0.33 x 10^4	9.15 ± 0.26 x 10^4	6.91 ± 0.26 x 10^4	9.35 ± 0.84 x 10^4
n (binding stoichiometry, HSA: EFHB)	1.11 ± 0.01	1.10 ± 0.01	1.17 ± 0.01	1.10 ± 0.01
ΔG (Gibbs free energy change, kcal mol^{-1})	-6.67 ± 0.03	-6.76 ± 0.03	-6.72 ± 0.04	-7.05 ± 0.05

The data are the average with standard deviation of three independent trials.

UV-Vis absorption spectroscopy technique is a simple method to determine structural changes due to the formation of complexes. In order to confirm the results obtained by Stern-Volmer and quenching bimolecular constant (Table 3), the UV-vis absorption spectra of the HSA, EFHB and the HSA-EFHB complex were determined (Figure 7).[4,22,42,43] Dynamic mechanism only affects the excited states of the fluorophores, therefore no change in the absorption spectrum is expected, contrary to this the formation of a complex that gives rise to a quenching by mechanism static should manifest itself with changes in the absorption spectrum of the biomolecule.[35,37]

Figure 7 shows the HSA absorption spectrum (spectrum A, maximum absorbance at 280 nm), the resulting spectrum from the subtraction of the EFHB spectrum (spectrum C) to the absorption spectrum of the HSA-EFHB complex (Spectrum B), that showed an increase in the absorption intensity over the range of the absorption spectrum studied (250 to 500 nm, spectrum D) with respect to the spectrum of HSA in the absence of EFHB. Spectral changes found by the UV-Vis spectroscopic technique confirm the presence of complex formation. Therefore, the process of quenching the fluorescence of HSA interacting with EFHB is mediated primarily by a static mechanism.[4,5,44–46]

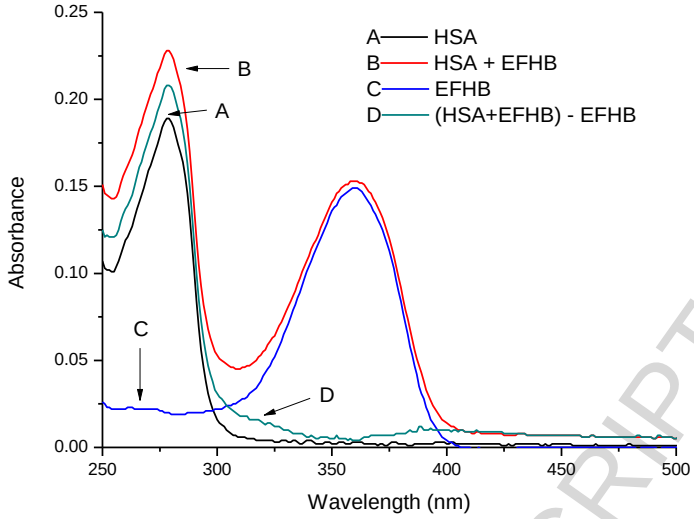

Figure 7. UV-vis absorption spectra of A) HSA, B) HSA + EFHB, C) EFHB and D) (HSA + EFHB) – EFHB; [HSA] = [EFHB] = 5.0 x 10^{-6} M.

3.6. Association constant and number of interaction sites.

As discussed above, the observed fluorescence quenching is typical static quenching, a modified Stern-Volmer equation (Equation 3) is applied to determine the affinity constant (K_a) for the system HSA-EFHB.[44,47]

$$\frac{F_O}{\Delta F} = \frac{F_O}{F_O - F} = \frac{1}{f_a K_a}\frac{1}{[Q]} + \frac{1}{f_o} \qquad (3)$$

Here, f_a stands for the fraction of accessible fluorescence and K_a is the effective quenching constant. F_0 and F are the corrected emission intensity of HSA in the absence and presence of quencher [Q] respectively, $F_0/\Delta F$ is linear with the reciprocal value of the quencher concentration [Q] (Figure 8), with slope equal to the value of $(f_a K_a)^{-1}$. K_a can be obtained from the intercept and slope. The corresponding values of K_a are listed in Table 3.[47] The K_a values for EFHB are 10^4 L mol^{-1}, suggesting very strong binding to HSA at the range of temperature studied. The K_a values obtained in the present study are consistent with previous literature reports to systems HSA-Hydrazones.[4–7]

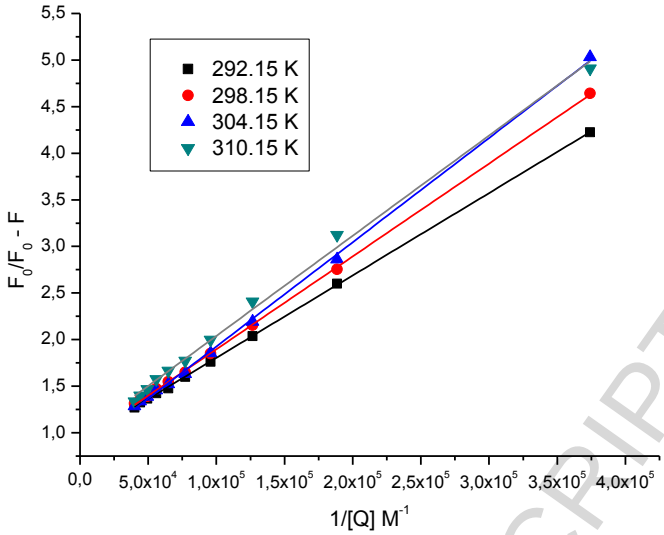

Figure 8. The plots of F_0/F *Vs* 1/[*Q*] for EFHB binding with HSA at various temperatures.

The number of bound complex HSA-EFHB (*n*) were determined by plotting the double *log* graph of the fluorescence data using.[47] Plotting $log((F_0 - F)/F)$ *Vs* $log[Q]$ according to equation 4, it was obtained a straight line whose slope denotes the number of interaction sites that may have in the formation of the HSA-EFBH complex (Figure 9).[42,43] The number of interaction sites for HSA-EFHB complex at different temperatures is approximately n = 1 (Table 3), meaning that only one molecule of the EFHB binds to one HSA molecule.[47]

$$log\frac{F_O - F}{F} = logK + nlog[Q] \qquad (4)$$

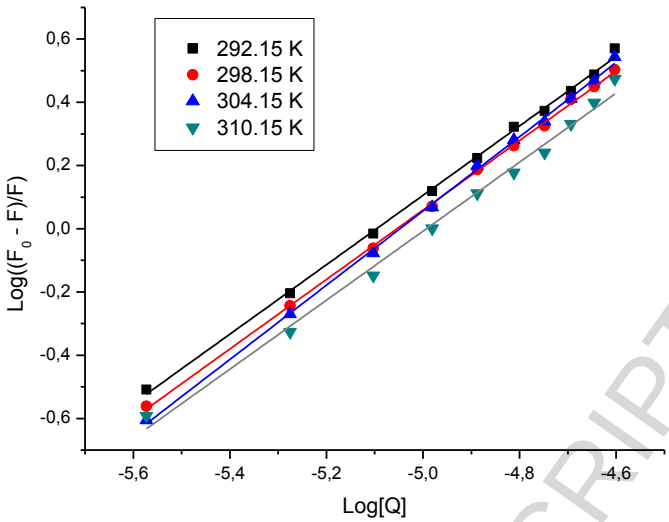

Figure 9. The plots of log((*F*$_0$ - *F*)/*F*) *Vs* log[*Q*] for EFHB binding with HSA at various temperatures.

3.7. Thermodynamic parameters.

Thermodynamic association parameters can be estimated by Gibbs-Helmholtz (Equation 5) and Van't Hoff isochore equations (Equation 6); these allow obtaining information about the magnitudes and the nature of the bond in the formation of ligand-biomolecule complexes. There are mainly four types of non-covalent interactions in the complex formation between small molecules and biomolecules, as such as hydrogen bonds, van der Waals forces, hydrophobic and electrostatic interactions.[32,48]

$$\Delta G = \Delta H - T\Delta S = -RTlnK_a \qquad (5)$$

$$\ln\left(\frac{K_{a2}}{K_{a1}}\right) = \left(\frac{1}{T_1} - \frac{1}{T_2}\right)\frac{\Delta H}{R} \qquad (6)$$

ΔG, ΔH and *ΔS* are the free energy of Giggs, enthalpy and entropy respectively, K_a is the constant of association to the temperature *T* and *R* is the constant of the gases. Ross and Subramanian reported an analysis of the thermodynamic parameters associated with the different types of interaction that can take place in the formation of ligand-biomolecule complexes.[48] The authors showed that, when:

- *ΔH* < 0 or *ΔH* ≅ 0 and *ΔS* > 0, the electrostatic forces are mainly involved in the complex formation process.

- $\Delta H < 0$ and $\Delta S < 0$, the interaction is dominated mainly by van der Waals forces or by hydrogen bonds.
- $\Delta H > 0$ and $\Delta S > 0$, the main interaction forces that give rise to the formation of the complex are the hydrophobic ones.

In this work, all HSA-EFHB association processes in the temperature range studied were spontaneous (Table 3). In the process of formation of the EFHB-HSA complex from 292.15 to 298.15 K it presented a ΔH = -2.72 kcal mol^{-1} and ΔS = 13.55 cal mol^{-1} K^{-1}, to the process from 298.15 to 304.15 K the values of ΔH was -5.50 kcal mol^{-1} and ΔS = 4.02 cal mol^{-1} K^{-1}, therefore, the process to the formation of the complex was more exothermic and with less favorable steric factors to the previous binding process (292.15-298.15 K), and into the increased temperature from 304.15 to 310.15 K, the values of ΔH and ΔS were -0.72 kcal mol^{-1} and 20.43 mol cal^{-1} K^{-1} respectively, for this case, the bonding process happened to be less exothermic and to be favored or sterically driven.[10,32,48]

Table 4. Thermodynamic parameters of the HSA-EFHB interaction at different temperatures.

Temperature (K)	ΔH (kcal mol^{-1})	ΔG (kcal mol^{-1})	ΔS (cal mol^{-1} K^{-1})
292.15-298.15	-2.72	-6.76	13.55
298.15-304.15	-5.50	-6.72	4.02
304.15-310.15	-0.72	-7.05	20.43

According to Ross and Subramanian, the association between HSA and EFHB in the temperature range studied is mainly mediated by electrostatic interactions, $\Delta H < 0$ and $\Delta S > 0$.[48]

3.8. Molecular modeling.

In this study, molecular docking was used to predict the binding constant and binding's site on HSA-EFHB complex to confirm the results of the experimental measurements described earlier, and to identify the main amino acid residues as well as the principal forces involved in the association HSA-EFHB. The best conformation of ligand with lowest binding-free energy (-7.32 kcal mol^{-1}) was in the subdomain IIA (Figure 10).

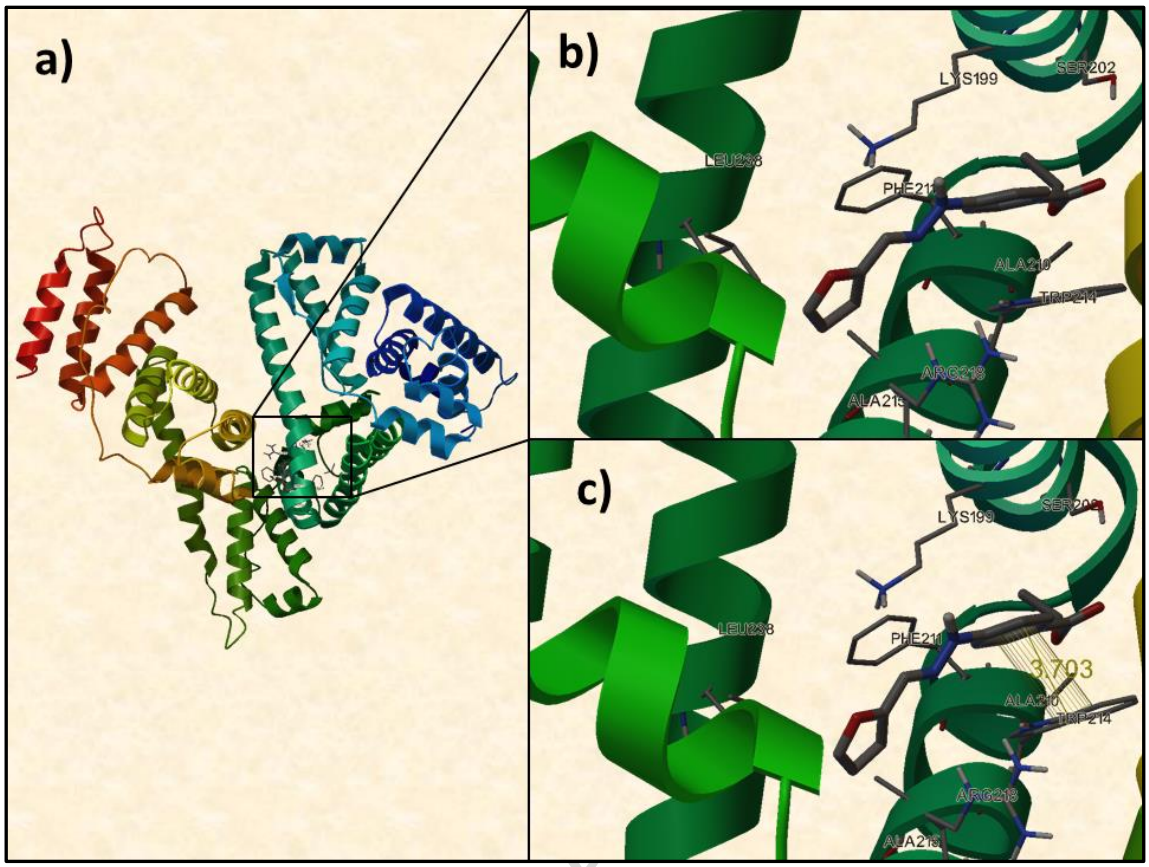

Figure 10. a) Union site, b) Specific and non-specific interactions and c) Interactions π-π of EFHB-HSA complex.

Molecular docking results also suggested hydrophobic and electrostatic interactions as the main binding forces, which is in accord to the experimental data. The complex HSA-EFHB is stabilized by stacking π...π with the residue Trp214 (distance 3.703 Å). On the other hand, EFHB is stabilized into HSA by hydrophobic interaction with the residues Lys199, Ser202, Ala210 and Ala215, Phe211, Arg218 and Leu238 (Figure 12). The calculated binding Gibbs, was ΔG = -7.32 kcal mol^{-1}; while the experimental data was -6.79 kcal mol^{-1}, this can be attributed to the differences between the X-ray structures of the protein from crystals to the aqueous system used in this study.

6. Conclusions

This paper describes the synthesis and characterization of the substituted phenylhydrazone derivative EFHB using different spectroscopic techniques, along with a single-crystal X-ray structure, and the reaction between of HSA and EFHB which was investigated using spectroscopic fluorescence and molecular modeling methods. The

intrinsic fluorescence of HSA was quenched by EFHB with static quenching mechanism. The association constants, number of binding sites and thermodynamic parameters were determined at different temperatures. In addition, binding site was located at the subdomain IIA of HSA. The binding study of drugs with proteins is of great importance in pharmacy, pharmacology, and biochemistry. This study is expected to provide important insight into the interactions of the physiologically important protein HSA with drugs.

Acknowledgments

The authors thank Fondo Nacional de Ciencia, Tecnología e Innovación (FONACIT Proyecto de apoyo a Grupos No. G-2005000403). Proyecto 1063, Instituto Venezolano de Investigaciones Científicas (IVIC).

References

[1] N.P. Belskaya, W. Dehaen, V.A. Bakulev, Synthesis and properties of hydrazones bearing amide, thioamide and amidine functions, Arkivoc. 2010 (2010) 275–332. doi:10.3998/ark.5550190.0011.108.

[2] A.-Z.A. Elassar, H.H. Dib, N.A. Al-Awadi, M.H. Elnagdi, Chemistry of carbofunctionally substituted hydrazones., Ark. (Gainesville, FL, United States). 2007 (2007) 272–315. doi:10.3998/ark.5550190.0008.210.

[3] S. Rollas, Ş.G. Küçükgüzel, Biological activities of hydrazone derivatives, Molecules. 12 (2007) 1910–1939. doi:10.3390/12081910.

[4] F.F. Tian, F.L. Jiang, X. Le Han, C. Xiang, Y.S. Ge, J.H. Li, Y. Zhang, R. Li, X.L. Ding, Y. Liu, Synthesis of a novel hydrazone derivative and biophysical studies of its interactions with bovine serum albumin by spectroscopic, electrochemical, and molecular docking methods, J. Phys. Chem. B. 114 (2010) 14842–14853. doi:10.1021/jp105766n.

[5] F.F. Tian, J.H. Li, F.L. Jiang, X. Le Han, C. Xiang, Y.S. Ge, L.L. Li, Y. Liu, The adsorption of an anticancer hydrazone by protein: An unusual static quenching mechanism, RSC Adv. 2 (2012) 501–513. doi:10.1039/c1ra00521a.

[6] J.Q. Tong, F.F. Tian, Q. Li, L.L. Li, C. Xiang, Y. Liu, J. Dai, F.L. Jiang, Probing the adverse temperature dependence in the static fluorescence quenching of BSA induced by a novel anticancer hydrazone, Photochem. Photobiol. Sci. 11 (2012) 1868–1879. doi:10.1039/c2pp25162k.

[7] J.Q. Tong, F.F. Tian, Y. Liu, F.L. Jiang, Thermodynamic properties of the site-selective binding of a bromo-hydrazone and its unsubstituted analogue to human serum albumin, J. Solution Chem. 44 (2015) 193–205. doi:10.1007/s10953-015-0303-7.

[8] O.K. Abou-Zied, O.I.K. Al-Shihi, Characterization of Subdomain IIA Binding Site of Human Serum Albumin in its Native, Unfolded, and Refolded States Using Small Molecular Probes, J. Am. Chem. Soc. 130 (2008) 10793–10801. doi:10.1021/ja8031289.

[9] O.K. Abou-Zied, N. Al-Lawatia, Exploring the Drug-Binding Site Sudlow I of Human Serum Albumin: The Role of Water and Trp214 in Molecular

Recognition and Ligand Binding, ChemPhysChem. 12 (2011) 270–274. doi:10.1002/cphc.201000742.

[10] S. Bi, L. Yan, Y. Sun, H. Zhang, Investigation of ketoprofen binding to human serum albumin by spectral methods, Spectrochim. Acta Part A Mol. Biomol. Spectrosc. 78 (2011) 410–414. doi:10.1016/j.saa.2010.11.002.

[11] M. Bagheri, M.H. Fatemi, Fluorescence spectroscopy, molecular docking and molecular dynamic simulation studies of HSA-Aflatoxin B1 and G1 interactions, J. Lumin. 202 (2018) 345–353. doi:10.1016/j.jlumin.2018.05.066.

[12] G. Rabbani, M.H. Baig, A.T. Jan, E.J. Lee, M.V. Khan, M. Zaman, A. Farouk, R.H. Khan, I. Choi, Binding of erucic acid with human serum albumin using a spectroscopic and molecular docking study, Int. J. Biol. Macromol. 12 (2017) 979–990. doi:10.1016/j.ijbiomac.2017.04.051.

[13] M. Ishtikhar, G. Rabbani, S. Khan, R.H. Khan, RSC Advances Biophysical investigation of thymoquinone binding, RSC Adv. 5 (2015) 18218–18232. doi:10.1039/C4RA09892G.

[14] A. Varshney, M. Rehan, N. Subbarao, G. Rabbani, R.H. Khan, Elimination of Endogenous Toxin , Creatinine from Blood Plasma Depends on Albumin Conformation : Site Specific Uremic Toxicity & Impaired Drug Binding, PLoS One. 6 (2011) e17230. doi:10.1371/journal.pone.0017230.

[15] M. Morales-Toyo, Y.J. Alvarado, J. Restrepo, L. Seijas, R. Atencio, J. Bruno-Colmenarez, Synthesis, Crystal Structure Analysis, Small Cluster Geometries and Energy Study of (E)-Ethyl-4-(2-(thiofen-2-ylmethylene)hydrazinyl)benzoate, J. Chem. Crystallogr. 43 (2013) 544–549. doi:10.1007/s10870-013-0455-5.

[16] ACD/ChemSketch, Freeware version 10.00, Adv. Chem. Dev. Inc., Toronto, ON, Canada. (2006). www.acdlabs.com.

[17] Bruker, SAINT. Bruker AXS Inc., Madison, Wisconsin, USA., (2009).

[18] G.M. Sheldrick, Crystal structure refinement with SHELXL, Acta Crystallogr. Sect. C Struct. Chem. 71 (2015) 3–8. doi:10.1107/S2053229614024218.

[19] A.L. Spek, Structure validation in chemical crystallography, Acta Crystallogr. Sect. D Biol. Crystallogr. 65 (2009) 148–155. doi:10.1107/S090744490804362X.

[20] I. Choi, K. Ahmad, M.H. Baig, G. Rabbani, E.J. Lee, Binding of Tolperisone Hydrochloride with Human Serum Albumin: Effects on the Conformation, Thermodynamics, and Activity of HSA, Mol. Pharm. 15 (2018) 1445–1456. doi:10.1021/acs.molpharmaceut.7b00976.

[21] C.M. Fernández, V.C. Martin, Preparation d'un tampon universel de force ionique 0,3 M, Talanta. 24 (1977) 747–748. doi:10.1016/0039-9140(77)80204-X.

[22] A. Varlan, M. Hillebrand, Bovine and Human Serum Albumin Interactions with 3-Carboxyphenoxathiin Studied by Fluorescence and Circular Dichroism Spectroscopy, Molecules. 15 (2010) 3905–3919. doi:10.3390/molecules15063905.

[23] O. Trott, A.J. Olson, Software News and Update AutoDock Vina: Improving the Speed and Accuracy of Docking with a New Scoring Function, Efficient Optimization, and Multithreading, J. Comput. Chem. 31 (2010) 455–461. doi:10.1002/jcc.

[24] J. Ghuman, P.A. Zunszain, I. Petitpas, A.A. Bhattacharya, M. Otagiri, S. Curry, Structural basis of the drug-binding specificity of human serum albumin, J. Mol. Biol. 353 (2005) 38–52. doi:10.1016/j.jmb.2005.07.075.

[25] G.M. Morris, R. Huey, W. Lindstrom, M.F. Sanner, R.K. Belew, D.S. Goodsell, A.J. Olson, CHARMM: The Biomolecular Simulation Program B., J. Comput. Chem. 30 (2009) 1545–1614. doi:10.1002/jcc.

[26] Z. Bikadi, E. Hazai, Application of the PM6 semi-empirical method to modeling proteins enhances docking accuracy of AutoDock, J. Cheminform. 1 (2009) 1–16. doi:10.1186/1758-2946-1-15.
[27] and D.J.F. M. J. Frisch, G. W. Trucks, H. B. Schlegel, G. E. Scuseria, M. A. Robb, J. R. Cheeseman, G. Scalmani, V. Barone, B. Mennucci, G. A. Petersson, H. Nakatsuji, M. Caricato, X. Li, H. P. Hratchian, A. F. Izmaylov, J. Bloino, G. Zheng, J. L. Sonnenberg, M. Had, Gaussian 09 Rev. D. 01, 01 (2009) 2009.
[28] C.R. Groom, I.J. Bruno, M.P. Lightfoot, S.C. Ward, feature articles The Cambridge Structural Database, Acta Crystallogr. Sect. B Struct. Sci. B72 (2016) 171–179. doi:10.1107/S2052520616003954.
[29] P.A. Wood, F.H. Allen, E. Pidcock, Hydrogen-bond directionality at the donor H atom — analysis of interaction energies and database statistics, CrystE. 11 (2009) 1563–1571. doi:10.1039/b902330e.
[30] L. Fábián, A. Kálmán, Volumetric measure of isostructurality, Acta Crystallogr. Sect. B Struct. Sci. 55 (1999) 1099–1108. doi:10.1107/S0108768199009325.
[31] J. Bernstein, R.E. Davis, L. Shimoni, N. -L Chang, Patterns in Hydrogen Bonding: Functionality and Graph Set Analysis in Crystals, Angew. Chemie Int. Ed. English. 34 (1995) 1555–1573. doi:10.1002/anie.199515551.
[32] S. Bi, H. Zhang, C. Qiao, Y. Sun, C. Liu, Studies of interaction of emodin and DNA in the presence of ethidium bromide by spectroscopic method, Spectrochim. Acta Part A Mol. Biomol. Spectrosc. 69 (2008) 123–129. doi:10.1016/j.saa.2007.03.017.
[33] M.S. Ali, H.A. Al-Lohedan, Spectroscopic and computational evaluation on the binding of safranal with human serum albumin: Role of inner filter effect in fluorescence spectral correction, Spectrochim. Acta - Part A Mol. Biomol. Spectrosc. 203 (2018) 434–442. doi:10.1016/j.saa.2018.05.102.
[34] B.P. Kamat, J. Seetharamappa, In vitro study on the interaction of mechanism of tricyclic compounds with bovine serum albumin, J. Pharm. Biomed. Anal. 35 (2004) 655–664. doi:10.1016/j.jpba.2004.02.008.
[35] C.B. Berde, B.S. Hudson, R.D. Simoni, L.A. Sklar, Human serum albumin spectroscopic studies of binding and proximity relationships for fatty acids and bilirubin, J. Biol. Chem. 254 (1979) 391–400. en.m.wikipedia.org/wiki/albumin.
[36] X.M. He, D.C. Carter, Atomic structure and chemistry of human serum albumin, Nature. 358 (1992) 209–215. doi:10.1038/358209a0.
[37] G. Sudlow, D.J. Birkett, D.N. Wade, The Characterization of Two Specific Drug Binding Sites on Human Serum, Mol. Pharmacol. 11 (1975) 824–832.
[38] J. Peuravuori, R. Koivikko, K. Pihlaja, Characterization, differentiation and classification of aquatic humic matter separated with different sorbents: synchronous scanning fluorescence spectroscopy, Water Res. 36 (2002) 4552–4562. doi:10.1016/S0043-1354(02)00172-0.
[39] Y. Wang, G. Zhang, L. Wang, Interaction of prometryn to human serum albumin: Insights from spectroscopic and molecular docking studies, Pestic. Biochem. Physiol. 108 (2014) 66–73. doi:10.1016/j.pestbp.2013.12.006.
[40] X.-M. Zhou, W.-J. Lü, L. Su, Z.-J. Shan, X.-G. Chen, Binding of Phthalate Plasticizers to Human Serum Albumin in Vitro: A Multispectroscopic Approach and Molecular Modeling, J. Agric. Food Chem. 60 (2012) 1135–1145. doi:10.1021/jf204380r.
[41] M.A. Cheema, P. Taboada, S. Barbosa, J. Juárez, M. Gutiérrez-Pichel, M. Siddiq, V. Mosquera, Human serum albumin unfolding pathway upon drug binding: A thermodynamic and spectroscopic description, J. Chem. Thermodyn. 41 (2009)

439–447. doi:10.1016/j.jct.2008.11.011.
[42] B. Chakraborty, S. Basu, Interaction of BSA with proflavin: A spectroscopic approach, J. Lumin. 129 (2009) 34–39. doi:10.1016/j.jlumin.2008.07.012.
[43] P. Daneshgar, A.A. Moosavi-Movahedi, P. Norouzi, M.R. Ganjali, A. Madadkar-Sobhani, A.A. Saboury, Molecular interaction of human serum albumin with paracetamol: Spectroscopic and molecular modeling studies, Int. J. Biol. Macromol. 45 (2009) 129–134. doi:10.1016/j.ijbiomac.2009.04.011.
[44] A.S. Sharma, S. Anandakumar, M. Ilanchelian, In vitro investigation of domain specific interactions of phenothiazine dye with serum proteins by spectroscopic and molecular docking approaches, RSC Adv. 4 (2014) 36267–36281. doi:10.1039/c4ra04630g.
[45] A.A. Saboury, C. Pillip, S. Riahi, B. Larijani, M. Hosseini, F. Faridbod, M.R. Ganjali, P. Norouzi, Interaction study of pioglitazone with albumin by fluorescence spectroscopy and molecular docking, Spectrochim. Acta Part A Mol. Biomol. Spectrosc. 78 (2010) 96–101. doi:10.1016/j.saa.2010.09.001.
[46] M.S. Seyed Dorraji, V. Panahi Azar, M.H. Rasoulifard, Interaction between deferiprone and human serum albumin: Multi-spectroscopic, electrochemical and molecular docking methods, Eur. J. Pharm. Sci. 64 (2014) 9–17. doi:10.1016/j.ejps.2014.08.001.
[47] S. Tabassum, W.M. Al-Asbahy, M. Afzal, F. Arjmand, Synthesis, characterization and interaction studies of copper based drug with Human Serum Albumin (HSA): Spectroscopic and molecular docking investigations, J. Photochem. Photobiol. B Biol. 114 (2012) 132–139. doi:10.1016/j.jphotobiol.2012.05.021.
[48] P.D. Ross, S. Subramanian, Thermodynamics of protein association reactions: forces contributing to stability, Biochemistry. 20 (1981) 3096–3102. doi:10.1021/bi00514a017.

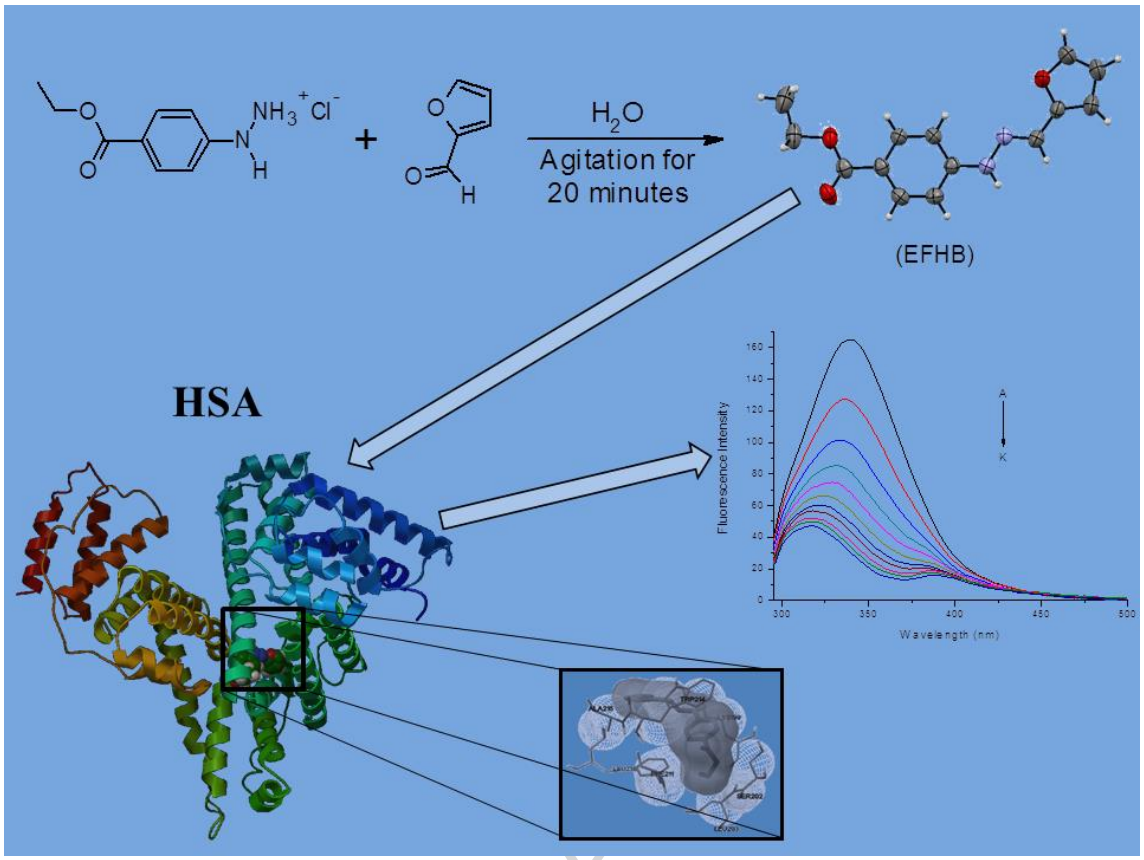

Graphical abstract

Highlights (EFHB)

.- A new phenylhydrazone derivative was synthesized.

.- The influence of the EFBH on the emission spectrum of the HSA was studied.

.- The HSA-EFHB association occurs through a static mechanism or complex formation.

.- The binding site of EFHB in the HSA was studied using molecular modeling.